UCLA

Title
Thermoresponsive Copolypeptide Hydrogel Vehicles for Central Nervous System Cell Delivery.

Permalink
https://escholarship.org/uc/item/3f56x19n

Journal
ACS biomaterials science & engineering, 1(8)

ISSN
2373-9878

Authors
Zhang, Shanshan
Burda, Joshua E
Anderson, Mark A
et al.

Publication Date
2015-08-01

DOI
10.1021/acsbiomaterials.5b00153

Peer reviewed

Thermoresponsive Copolypeptide Hydrogel Vehicles for Central Nervous System Cell Delivery

Shanshan Zhang,[†,⊥] Joshua E. Burda,[‡,⊥] Mark A. Anderson,[‡,⊥] Ziru Zhao,[‡] Yan Ao,[‡] Yin Cheng,[§] Yi Sun,[§] Timothy J. Deming,[†,∥] and Michael V. Sofroniew*,[‡]

[†]Department of Chemistry and Biochemistry, [‡]Department of Neurobiology and [§]Department of Psychiatry and Biobehavioral Sciences, David Geffen School of Medicine, and [∥]Department of Bioengineering, University of California, Los Angeles, California 90095, United States

ABSTRACT: Biomaterial vehicles have the potential to facilitate cell transplantation in the central nervous system (CNS). We have previously shown that highly tunable ionic diblock copolypeptide hydrogels (DCH) can provide sustained release of hydrophilic and hydrophobic molecules in the CNS. Here, we show that recently developed nonionic and thermoresponsive DCH, called DCH_T, exhibit excellent cytocompatibility. Neural stem cell (NSC) suspensions in DCH_T were easily injected as liquids at room temperature. DCH_T with a viscosity tuned to prevent cell sedimentation and clumping significantly increased the survival of NSC passed through injection cannulae. At body temperature, DCH_T self-assembled into hydrogels with a stiffness tuned to that of CNS tissue. After injection in vivo, DCH_T significantly increased by 3-fold the survival of NSC grafted into a healthy CNS. In an injured CNS, NSC injected as suspensions in DCH_T distributed well in non-neural lesion cores, integrated with healthy neural cells at lesion perimeters, and supported regrowing host nerve fibers. Our findings show that nonionic DCH_T have numerous advantageous properties that make them useful tools for in vivo delivery of cells and molecules in the CNS for experimental investigations and potential therapeutic strategies.

KEYWORDS: biomaterials, hydrogel, brain, spinal cord, drug delivery, neural stem cells, transplantation
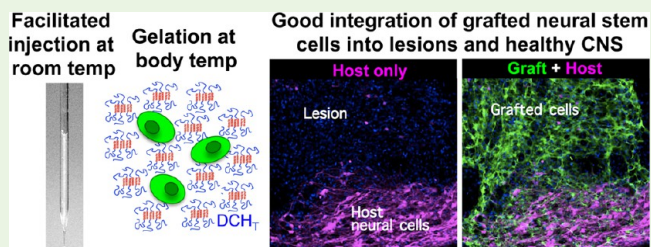
1. INTRODUCTION

Transplantation into the central nervous system (CNS) of neural stem cells (NSCs) and other cells is under intense investigation as a potential means of facilitating neural repair and replacing lost connections in CNS disorders such as traumatic injury, stroke, or degenerative disease.[1−4] Cell transplantation into the CNS would benefit from vehicles that enhance cell viability during the injection procedure, optimize cell distribution, and could deliver different types of molecules that might facilitate and regulate the maturation of transplanted cells as well as their integration and interactions with host cells. Biomaterial-based vehicles have the potential to enhance the efficacy of CNS cell transplantation in all of these ways. Numerous biomaterials, including natural and synthetic materials, are being investigated for this purpose. For example, fibrin matrix is a natural material formed by mixing fibrinogen and thrombin, which rapidly interact and entrap cells and added molecules in clot-like structures that are reportedly useful in retaining grafted cells at injection sites.[2] Nevertheless, the rapid clotting of fibrin can complicate delivery procedures, and both thrombin and fibrin are endogenous blood-borne molecules with powerful signaling properties that affect multiple cell types at sites of CNS injury.[5] Exposure to these or other incompletely identified bioactive molecules that may be contained within natural materials used as transplant vehicles may result in effects that are unexpected or may not be desirable and could distort the function of graft or host cells. The ability to generate vehicles whose components are fully known and characterized has advantages both for experimental studies and for potential clinical translation.

Hydrogels that can be injected and then form local depots represent a promising means of achieving sustained local delivery of different types of molecules in the CNS[6,7] and also have the potential to serve as vehicles for cell transplantation.[8,9] Hydrogels that are suitable for CNS applications will need to exhibit physical properties such as rigidity, porosity, and surface chemistry that are compatible with CNS tissue as well as be able to deliver a variety of functional components.[10] Hydrogels are available from naturally occurring or synthetic sources. Fully synthetic biomaterials that are functionally inert but can be intentionally functionalized with well-characterized molecules for specific contexts offer advantages as vehicles and carriers for CNS cell transplantation.[10] In addition, because the types of physical properties and functional components that will be required of vehicles are incompletely characterized for CNS tissue in the context of injury or disease, there is a need for versatile materials that can be easily tuned to meet the

requirements of specific applications and modified in accordance with practical experience.

Diblock copolypeptide hydrogels (DCH), composed of discrete hydrophilic and hydrophobic segments, are amphiphilic synthetic materials with many features that make them attractive for CNS applications that are likely to require progressive adjustment and fine-tuning of material properties.[11] A combination of chemical synthesis and structural characterization has provided a detailed understanding of DCH structure−property relationships that allow a high level of control over gel stiffness, gel porosity, gel functionality, and media stability, and many of these properties can be adjusted independently of each other.[12−14] Based on information from these prior studies, DCH physical properties can be varied readily and predictably by altering copolymer chain length, architecture, or composition,[11] and DCH, therefore, have the potential for continual refinement, incremental optimization, and fine-tuning in response to experimental or clinical experience. We previously showed that, after injection in vivo, DCH self-assemble into discrete, well-formed deposits of semirigid gel networks that integrate well with host CNS tissue, cause no detectable toxicity or adverse inflammatory reaction, and are fully degraded after several months in vivo.[10] In addition, DCH depots placed into the healthy or injured CNS can provide several weeks of sustained local release of both hydrophilic and hydrophobic effector molecules.[7,15] Thus, DCH depots can efficiently provide sustained, local delivery within the CNS of a broad spectrum of bioactive and potentially therapeutic molecules, ranging from diverse proteins to small hydrophobic drug candidates.

Hydrogels whose gelling behavior is regulated by temperature can offer advantages for in vivo delivery.[16,17] We recently extended the utility of DCH for CNS applications by developing nonionic and thermoresponsive DCH, called DCH_T, that are liquid at room temperature (22 °C) and form semirigid gels at just below body temperature (33−35 °C).[18] DCH_T exhibit excellent cytocompatibility and support the long-term viability of suspended cells in vitro, while retaining the many advantageous features of our previously studied ionic DCH, such as injectability, tunable rigidity and porosity, and the ability to load and provide sustained release of both hydrophilic and hydrophobic molecules.[18] In the study reported here, we tested and characterized nonionic and thermoresponsive DCH_T with respect to their properties and effects on CNS tissue after injections in vivo, with regard to their potential to support and increase the survival of NSC during grafting procedures, as well as to improve NSC integration and interactions with host cells after transplantation into the healthy and injured CNS.

2. METHODS

2.1. Preparation of DCH_T. DCH_T samples were manufactured as previously described,[18] with average total lengths of around 200 residues, and contained either poly(L-leucine), L, or poly(γ-[2-(2-methoxyethoxy)ethyl]-L-glutamate-stat-L-leucine), E^{P2}/L, as the hydrophobic domain, and poly(γ-[2-(2-methoxyethoxy)ethyl]-rac-glutamate), rac-E^{P2}, as the hydrophilic domain. Briefly, DCH_T were synthesized by sequential copolymerization of desired NCA monomers using the transition metal initiator $Co(PMe_3)_4$ in tetrahydrofuran according to published procedures.[13] All copolymerization reactions were performed in a dinitrogen-filled glovebox using anhydrous solvents. Isolated yields of the purified copolymers ranged between 90 and 95%. Relative copolypeptide compositions were determined using ^1H NMR and were found to be within 1% of predicted values.

Based on previously described in vitro observations,[18] we determined that an optimized nonionic DCH_T formulation for in vivo testing consisted of a blend of $(rac\text{-}E^{P2})_{180}(E^{P2}_{0.5}/L_{0.5})_{30}$ admixed with $(rac\text{-}E^{P2})_{180}(L)_{30}$ in an equimolar ratio, designated here as DCH_T. This DCH_T blend at 3% concentration gave efficient loading and sustained release of both hydrophilic and hydrophobic cargo in vitro[18] and gelation just below normal body temperature. DCH_T was used for the extensive in vivo testing and characterization described in the present study.

For certain experiments, DCH_T was mixed with a small amount of $K_{180}L_{30}$ (ref 10) conjugated with a fluorescent dye to track hydrogel location in vivo. Fluorescent tagging of lysine ε-amine groups was performed using AMCA-X [6-((7-amino-4-methylcoumarin-3-acetyl)-amino)hexanoic acid] (AnaSpec, cat# 81207) as a blue fluorescent tag, which was attached using NHS-EDC coupling chemistry. In this procedure, $K_{180}L_{30}$ powder (3.2 mmol) was dissolved in phosphate-buffered saline (PBS) (pH = 6.5, 30 mL, 0.1 M). To the polypeptide suspension were added 2 equiv of NHS (N-hydroxysuccinimide) in PBS (pH = 6.5), 10 equiv of EDC (1-ethyl-3-(3-(dimethylamino)-propyl)carbodiimide) in PBS (pH = 6.5), and 1 equiv of AMCA-X in dimethylsulfoxide per copolypeptide chain (corresponding to 2.8% of the available lysine amines), and the mixture was stirred for 16 h. For purification, the sample was covered in aluminum foil to protect from light and then dialyzed (MWCO = 2 kDa) for 5 days against pyrogen-free water, with dialyzate changes every 12 h. The tagged polymer (AMCA-X-$K_{180}L_{30}$) was isolated by lyophilization. For use in injections in vivo, AMCA-X-$K_{180}L_{30}$ was mixed with DCH_T samples at a molar ratio of 1:10, respectively.

2.2. Neural Stem Cells for In Vitro Evaluations and In Vivo Transplantation. Primary NSCs were prepared as floating neurospheres[19,20] from forebrains of embryonic day 11 (E11) CD1 mice.[21] Telencephalon dissected from E11 embryos was first coarsely dissociated by mechanical force then treated with Papain (Worthington) for 5 min at 37 °C with constant shaking. Dissociated cells (3 × 10^6) were then plated onto polyornithine-coated (PO, Sigma) and fibronectin-coated (FN, Sigma) 10 cm dishes in serum-free medium containing DMEM/F12 (Invitrogen), 1% B27 (Invitrogen), and penicillin−streptomycin (50 $\mu g/mL$ and 50 U/mL, respectively). Cells were fed daily with basic fibroblast growth factor (bFGF, PeproTech) at a final concentration of 10 ng/mL. After confluence was reached, NSCs were passaged with enzymatic dissociation using StemPro Accutase (Invitrogen) and replated on PO/FN-coated tissue culture-treated plastic at a density of 1−2 × 10^6 cells per 10 cm dish and propagated until use in in vitro or in vivo experiments.

2.3. Three-Dimensional Culture of NSC in DCH_T. Primary NSCs prepared as above (section 2.2) were dissociated and resuspended at a final concentration of 200 000 cells/mL in either serum-free culture medium (DMEM/F12, Invitrogen) or in 2 or 3% DCH_T (w/v) prepared in DMEM/F12. Resuspended NSCs were transferred to the wells of 96-well cell culture plates or to dialysis cassettes with membrane molecular weight cutoff of 20 kDa and a 0.5 mL sample volume (Thermo Scientific-Pierce, Rockford IL, no. 87734, Slide-A-lyzer) and cultured in a 37 °C humidified atmosphere with 5% CO_2. Dialysis cassettes containing cells in DCH_T or control cells were submerged in media at 37 °C and incubated for 7 days, and the external medium was replaced every 2 days. At desired time points, NSCs were harvested and cell viability was determined using the MTS assay (see section 2.4).

2.4. In Vitro Cell Viability Assay. The viability of cells maintained under different conditions in vitro was quantified using the Cell Titer 96 aqueous nonradioactive cell proliferation assay (MTS assay) (Promega, Madison, WI).[22] For cells cultured in 96-well plates, the culture plates were centrifuged briefly and the cell culture medium was aspirated. For cells cultured in dialysis cassettes, 100 μL of cell suspension was transferred into a 96-well cell culture plate and centrifuged briefly to allow aspiration of the cell culture medium. Fresh medium containing 20% MTS solution was then added to the cells, which were then transferred to a humidified 5% CO_2 incubator at 37

°C for 1 h. Absorbance at 490 nm (A490) was measured for each well using an Infinite F200 plate reader (Tecan Systems Inc., San Jose, CA, USA). The background absorbance was read at 700 nm (A700) and subtracted from A490. The relative survival of the cells was quantified by taking the ratio of the (A490 − A700) values and comparing the experimental and control cells.

2.5. Cell Settlement Measurements. NSCs prepared as described above (section 2.2) were suspended in media or in 2 or 3% DCH_T at 200 000 cells/mL and transferred to 1 mL quartz cuvettes. The transmittance of light through the quartz cuvette at different time points was measured using a PerkinElmer Lambda EZ210 (λ = 500 nm). Since suspended cells scatter visible light, an increase in sample light transmittance or a decrease in light scattering indicates settling of cells out of the light path due to gravity. For visual evaluation of cell settlement in glass injection cannulae, the same concentrations of cells were used as for in vivo injections, 200 000 cells/μL in either culture medium or DCH_T.

2.6. In Vivo Injections of DCH_T and NSC to Healthy or Injured CNS. *2.6.1. Preparation of NSC in DCH_T for In Vivo Transplantation.* Primary NSCs prepared as described above (section 2.2) were labeled with the reporter protein, green fluorescent protein (GFP), by using lentiviral vectors expressing fluorescent ZsGreen1 (pLVX, Clontech). For in vivo transplantation, NSCs were dissociated and resuspended at a final concentration of 200 000 cells/μL in either culture medium or DCH_T (section 2.1) and kept on ice for up to a maximum of 6 h until transplantation.

2.6.2. Animals. In vivo experiments were conducted using either wild-type or transgenic C57Bl6 mice from in-house breeding colonies. The transgenic mice used expressed the reporter protein tdTomato (tdT) selectively in astroglial cells that expressed glial fibrillary acid protein (GFAP). These transgenic reporter mice were used as hosts for stem cell transplantation experiments in which all host GFAP-expressing cells were labeled with tdT, including normal, reactive, and scar-forming astrocytes, so as to differentiate host from graft-derived GFP-labeled astroglial cells. To generate these mice, we obtained the ROSA-tdT Cre-recombinase reporter strain from JAX Laboratories (Bar Harbor, ME) (JAX strain B6.Cg-*Gt(ROSA)26Sortm9(CAG-tdTomato)Hze*/J, stock# 007909). These highly efficient ROSA-tdT mice[23] were crossed with our mouse-GFAP-Cre mice line 73.12, which selectively and specifically target Cre-mediated loxP recombination to GFAP-expressing astroglia throughout the CNS, including after spinal cord injury.[24−26] Offspring of this cross that expressed both transgenes were referred to as mGFAP-Cre-tdT reporter mice. Mice were housed in a 12 h light/dark cycle in a specific pathogen-free (SPF) facility with controlled temperature and humidity and allowed free access to food and water, and all surgical procedures and experiments were conducted according to protocols approved by the Chancellor's Animal Research Committee of the Office for Protection of Research Subjects at UCLA.

2.6.3. Surgical Procedures. All surgical procedures were performed under sterile conditions with isoflurane in oxygen-enriched air as the general anesthesia and using an operating microscope (Zeiss, Oberkochen, Germany) and rodent stereotaxic apparatus (David Kopf, Tujunga, CA). Details of all surgical procedures have been published previously.[7,10,15,26,27] For injections into the caudate putamen nucleus, the skull was exposed and a burr hole was drilled with a high-speed dental drill. Sterile solutions of 2 μL of DCH_T or PBS, or NSC in DCH_T or culture medium, were injected stereotaxically into the center of the caudate putamen nucleus using the target coordinates of 0.5 mm anterior to Bregma, 2.0 mm lateral to Bregma, and a depth of 3.0 mm below the cortical surface. For injections into the spinal cord, mice were first given severe crush spinal cord injuries (SCI) using procedures described in detail elsewhere.[15,25−27] Briefly, after a dorsal laminectomy of a single vertebra, a severe crush injury was made at the level of the T9/T10 spinal cord by using no. 5 Dumont forceps (Fine Science Tools, Foster City, CA) that had been ground down to a tip width of 0.5 mm. These forceps were used without a spacer to fully compress the cord laterally from both sides for 5 s. Two days after SCI, 1 μL of NSC in DCH_T or culture medium was injected into the center of the clearly visible SCI

lesion immediately lateral to the central dorsal vein and to a depth of 0.6 mm below the spinal cord surface. All injections into the brain or spinal cord were made at a speed of 0.2 μL per minute using pulled glass micropipettes ground to a beveled tip with 150−250 μm i.d. connected via specialized connectors and high-pressure tubing (Kopf and Hamilton) to a 10 μL syringe (Hamilton) under the control of a microinfusion pump (Harvard Instruments). All animals were given analgesic immediately prior to surgery and every 12 h for at least 48 h postsurgery and thereafter as necessary. Some animals were given bromodeoxyuridine (BrdU, Sigma) to label dividing cells. BrdU was administered by intraperitoneal injections at 100 mg/kg dissolved in saline plus 0.007 N NaOH as a single daily injection for 6 days on days 2−7 after grafting.

2.7. Histological Procedures. At survival times of 7 or 21 days after forebrain or spinal cord injections, mice received terminal anesthesia by barbiturate overdose and were perfused transcardially with PBS followed by 10% formalin in PBS and processed for different types of histological procedures as described in detail elsewhere.[7,10,15,26,27] Brains or spinal cords were removed, postfixed overnight, and cryoprotected in buffered 30% sucrose for at least 2 days. Thirty or 40 μm coronal frozen sections were prepared using a cryostat microtome (Leica, Nussloch, Germany) and stained by immunohistochemistry. The primary antibodies used were rabbit anti-GFAP (1:2000 or 1:20000; Dako, Carpinteria, CA), goat anti-GFP (1:1000; Novus, Littleton, CO), rat anti-mouse CD45 (1:2000; BD Pharmingen, San Jose, CA), sheep anti-BrdU (1:6000; Maine Biotechnology Services, Portland, ME), rabbit anti-Iba1 (1:1000; Wako Chemicals, Richmond VA), rabbit anti-GSTπ (1:150; BD Pharmingen), mouse anti-NeuN (1:400 or 1:4000; Millipore Biosciences), and rabbit anti-neurofilament M (1:10000; BD Pharmingen). For bright-field microscopy, the developing agents used were biotinylated anti-rat and anti-rabbit secondary antibodies (Vector, Burlingame, CA), biotin−avidin−peroxidase complex (Vector), and diaminobenzidine (DAB, Vector). For cytoarchitecture, Nissl staining was conducted using cresyl violet according to standard procedures. For fluorescence microscopy, the developing agents used were anti-rat and anti-rabbit secondary antibodies conjugated to Alexa 488 (Molecular Probes) or to Cy3 or Cy5 (Vector Laboratories and Chemicon BD Pharmingen), and 4′,6′-diamidino-2-phenylindole dihydrochloride (DAPI; 2 ng/mL; Molecular Probes) was used as a general nuclear stain. Sections were coverslipped using ProLong Gold antifade reagent (Invitrogen, Grand Island, NY). Stained sections were examined and photographed using bright-field or fluorescence microscopy and scanning confocal laser microscopy (Zeiss, Oberkochen, Germany). Morphometric evaluations were conducted by tracing the graft perimeters and counting the cell densities of GFP-positive cells within grafts by using previously described image analysis procedures with NeuroLucida and StereoInvestigator (Microbrightfield, Williston, VT).[7,25−27]

3. RESULTS

3.1. Good Cytocompatibility of Neural Stem Cells in Nonionic DCH_T in Vitro. Our previous work indicated that the survival of mesenchymal stem cells incubated in nonionic DCH_T was equivalent to that in cell culture media over 48 h in vitro after gelation at 37 °C.[18] For the present study, we conducted studies to compare the viability of NSCs in nonionic DCH_T in vitro and in vivo. We used the same DCH_T blended formulation that we had previously tested extensively in vitro.[18] Briefly, this DCH_T formulation consists of a physical mixture of diblock copolypeptides of average total length of about 200 residues with discrete hydrophilic and hydrophobic segments. Hydrophilic domains contain poly(γ-[2-(2-methoxyethoxy)-ethyl]-*rac*-glutamate), *rac*-E^{P2}. Hydrophobic domains contain either poly(L-leucine), L, or poly(γ-[2-(2-methoxyethoxy)-ethyl]-L-glutamate-*stat*-L-leucine), E^{P2}/L. DCH_T was prepared as a blend of (*rac*-E^{P2})$_{180}$($E^{P2}_{0.5}$/L$_{0.5}$)$_{30}$ admixed with (*rac*-E^{P2})$_{180}$(L)$_{30}$ in an equimolar ratio (see section 2.1).

To determine the effects on cell viability of incubation of NSC in DCH_T over longer time periods after gelation at 37 °C in vitro, we used the neurosphere assay system.[19,20] In this well-characterized procedure, NSCs are propagated as floating colonies (neurospheres) suspended in culture media.[19,20] Neurospheres were prepared from embryonic NSCs according to standard procedures (see section 2.2), and NSCs were then passaged and resuspended in 3% DCH_T prepared in culture medium at room temperature and transferred into dialysis cassettes with a membrane molecular weight cutoff of 20 kDa. The entire dialysis cassettes were then immersed in culture media and incubat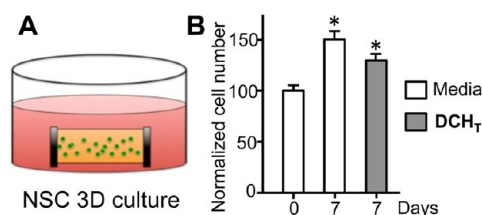ed at 37 °C (Figure 1A). This use of dialysis cassettes allowed the exchange of cell culture media at different time points without loss of DCH_T material, which can disperse into the media. The high molecular weight cutoff of the membrane allowed small molecules and most proteins to pass through but did not allow release of the DCH_T, which associated into a network. Dialysis cassettes containing NSC in media only served as controls. After incubation at 37 °C for 7 days, cell viability was measured using the MTS assay. NSC incubated in dialysis cassettes in either media alone or in DCH_T increased significantly in number over 7 days relative to the starting number of cells (Figure 1B), indicating continued proliferation of NSC, as expected. In addition, there was no significant difference in the number of cells after incubation in either media alone or DCH_T over 7 days (Figure 1B). These data demonstrate equivalent survival and proliferation of NSCs suspended in DCH_T compared with culture media alone.

3.2. Reduced Sedimentation of NSC Suspended in DCH_T during Injections. CNS transplantation requires injection of cells through fine-bore cannulae over prolonged injection times. The efficacy of injections can be hampered by the rapid sedimentation of cells suspended in low-viscosity aqueous vehicles. Cell sedimentation and clumping can lead to uneven grafting and can compromise cell viability by increasing shear stress during injection.[28,29] Grafting vehicles that have sufficient viscosity to delay sedimentation may be advantageous. DCH_T can be tuned to have a wide range of desired viscosities at ambient temperature by using blends without altering their ability to form semirigid gel networks above their gelation
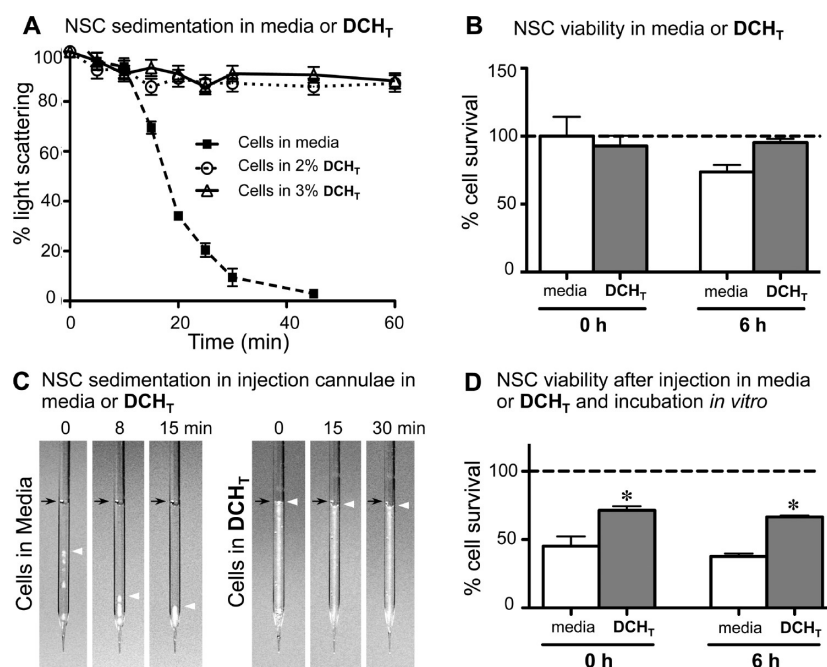

Figure 1. Viability of NSC suspended in DCH_T in vitro. (A) Schematic representation of NSC suspension within DCH_T for 3D culture in a 7 day study. (B) Numbers of NSCs increased significantly after culturing for 7 days in either cell culture media or DCH_T relative to the starting number of NSCs. There was no significant difference in the number of NSCs after culturing in cell culture media or DCH_T for 7 days. *$p < 0.001$ (ANOVA with post-hoc Newman−Keuls) ($n = 3$ cultures).

Figure 2. Sedimentation and viability of NSC in DCH_T after injection in vitro. (A) NSC (200 000 cells/mL) sedimentation in media or in different concentrations of optimized DCH_T as determined by scattered light transmittance ($\lambda = 500$ nm) at room temperature (22 °C). Light transmittance at time zero was measured immediately after achieving suspension of NSCs in either vehicle, and the inverse value was normalized to 100% light scattering. (B) Viability of NSC in either media or DCH_T after incubation on ice for 6 h to mimic normal handling conditions prior to in vivo injections. Time zero was measured immediately after harvesting of cell cultures and suspension of NSC in either vehicle. (C) Photographic images compare NSC (200 000 cells/μL) sedimentation in 2 μL of either media or DCH_T after loading injection cannulae (glass micropipettes) to model the in vivo injection procedure. Time zero was measured immediately after the 10 min required to load the pipettes with NSC in either vehicle. Note that considerable cell clumping and sedimentation occurred during the loading period with NSC in media. Black arrows indicate the top of the loaded vehicle. White arrowheads indicate the top of the suspended NSC. (D) Graph compares viability of NSC (200 000 cells/μL) suspended in either media or DCH_T after injection through pulled glass micropipettes (with beveled ground tips of 150−250 μm i.d.) over a 10 min period followed by incubation on ice for 0 or 6 h.
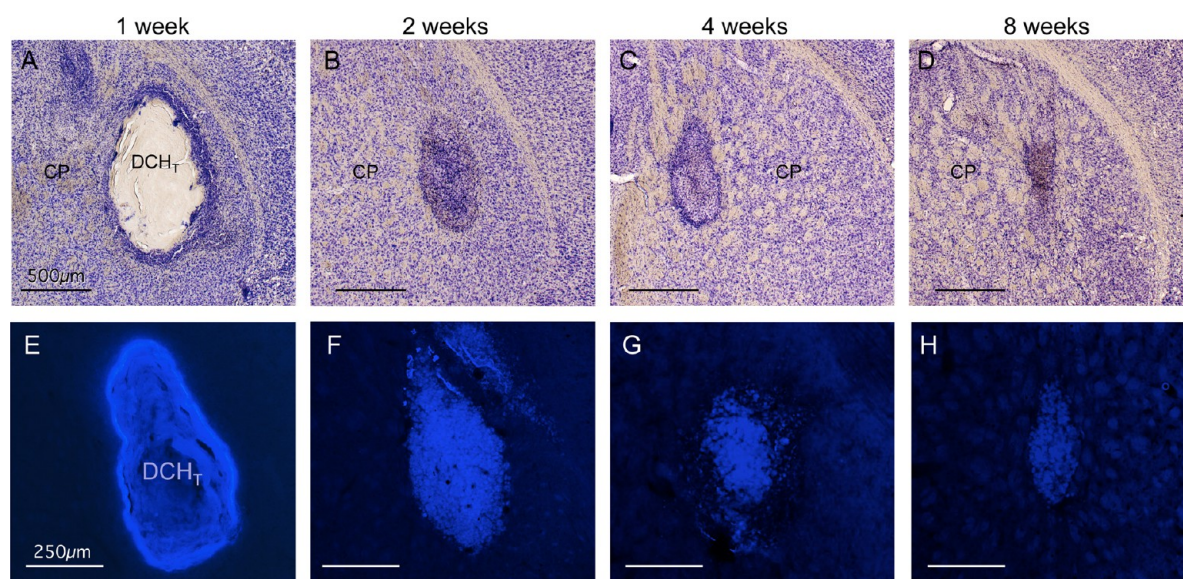
Figure 3. DCH_T injected into mouse forebrain self-assemble into well-formed deposits that are gradually absorbed over time. (A−D) Survey images of Nissl (cresyl violet)-stained mouse forebrain show typical DCH_T deposits at 1−8 weeks after injection into the caudate putamen (CP) nucleus (n = 4 mice per time point). Note the extensive intermingling of host cells with the DCH_T deposits between 1 week (A) and 2 weeks (B) after injection. (E−H) Higher-magnification images taken at the same time points show DCH_T deposits mixed with a small amount of blue fluorescent dye-labeled $K_{180}L_{30}$. Note the gradual diminution of deposit size (A−D) and loss of blue fluorescence labeling (E−H) over time, which are both indicative of gradual biodegradation and absorption of the DCH_T. Scale bars A−D = 500 μm, E−H = 250 μm.

temperature.[18] We therefore tested the ability of various DCH_T blends to delay the sedimentation of suspended NSCs by measuring the absorbance of scattered light, which decreases as cells settle out of the light path (Figure 2A). We found that the viscosity of our DCH_T blend[18] (see Methods) prepared in culture media at ambient temperature (22 °C) significantly delayed NSC sedimentation at both 2 and 3% concentrations (Figure 2A). Loss moduli (G'') are routinely used as an estimate of the viscous properties of hydrogels. Previous measurement of G'' of this DCH_T blend indicated G'' values at 1 Hz of about 18 Pascal at 2% and about 25 Pascal at 3% concentrations.[18] NSCs suspended in DCH_T at 22 °C gave stable suspensions that showed negligible sedimentation for up to 1 h (Figure 2A), whereas NSC suspended in standard culture media rapidly settled out of suspension (Figure 2A).

Cell transplantation procedures often require the storage of cells on ice for prolonged periods prior to CNS injection. We found that NSC viability did not diminish over 6 h while stored on ice while suspended in DCH_T prepared in culture media, and that viability of NSC stored in this manner was at least as good or better in comparison with NSC storage in culture media alone (Figure 2B).

We next examined the sedimentation of NSC after loading into the cannulae used for CNS injections. NSC suspended in culture media alone began to settle already during the process of drawing up the cell suspension into the glass micropipettes used for cell injections into the mouse CNS in vivo. These micropipettes are beveled to pointed tips with inner diameters of about 150−250 μm. By the end of the 10 min required to load 2 μL of injection volume at the rate of 0.2 μL/min used to load pipettes for in vivo injections, the NSC had routinely sedimented substantively to about halfway down the injection volumes and formed large visible clumps (time 0 in Figure 2C). After a further 8 min, which is less than the time required to correctly place and then complete a CNS injection in vivo, the majority of the NSC had sedimented into large visible clumps

at the bottom of micropipettes (Figure 2C). In striking contrast, NSCs suspended in 2% DCH_T prepared in culture media remained evenly dispersed throughout the entire injection volume and exhibited no detectable evidence of cell sedimentation throughout the period of loading micropipettes and for up to at least 30 min thereafter (Figure 2C), which would allow for ample time to position the micropipettes and complete injections in the absence of sedimentation.

3.3. Increased Survival of NSCs Suspended in DCH_T during Injections. We then evaluated the survival of NSC after they were passed through the injection micropipettes while being suspended in either cell culture media alone or in DCH_T prepared in culture media. Micropipettes were loaded with 2 μL of cell suspensions as above (section 3.2, Figure 2C), and cell suspensions were then immediately injected into cell culture wells at a rate of 0.2 μL/min, using the same conditions followed for in vivo injections. Injected cells were resuspended in culture media, and cell viability was determined immediately and after incubation for an additional 6 h. The viability of NSCs loaded and injected in culture media alone decreased by over 50% immediately after injection and fell further after incubation for 6 h on ice (Figure 2D). In contrast, the survival of NSCs loaded and injected DCH_T fell only by about 25% immediately after injection, and after incubation for a further 6 h, NSC survival after injection in DCH_T was significantly higher by almost double compared with survival after injection in media alone (Figure 2D). These findings show that DCH_T can significantly and substantively protect and enhance the survival of NSCs during the process of loading and injection through small-bore cannulae.

3.4. Properties of Nonionic DCH_T Injected into Healthy Mouse Forebrain. We next characterized the in vivo appearance, gelation, deposit formation, degradation time, and effects on host CNS tissue of DCH_T injected into healthy CNS of wild-type mice. Our previous measurements indicated that mouse forebrain tissue has a stiffness (storage modulus,

G') of about 190 Pascal[10] and that DCH in the G' range of about 50−120 Pascal formed discrete, well-tolerated deposits after injection into forebrain in vivo.[7,10] We selected the 3% DCH_T formulation used here for in vivo testing because of its G' of about 100 Pascal at body temperature.[18] We injected 2 μL volumes of 3% DCH_T into mouse forebrain and examined the tissue after survival times of 1, 2, 4, and 8 weeks (n = 4 mice per survival time) (Figures 3 and 4). Injections were made into the
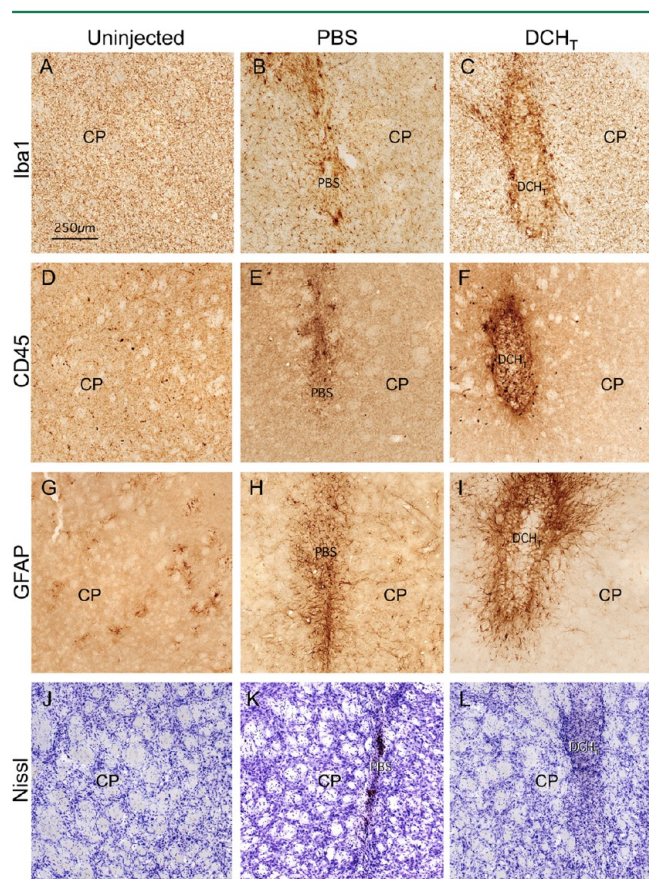

Figure 4. Reactive gliosis and inflammation are minimal and similar after injection of DCH_T or PBS into mouse forebrain. (A−L) Images show tissue sections through the caudate putamen (CP) nucleus either uninjected (A,D,G,J) or 8 weeks after local injection of PBS (B,E,H,K) or DCH_T (C,F,I,L), and immunohistochemically stained for multiple markers of gliosis and inflammation (A−I) or tissue architecture (J−L). Note that, compared with uninjected tissue, the reactive responses of different host cell types including microglia stained for Iba1 (A−C), infiltrating inflammatory cells stained for CD45 (D−F), and astrocytes stained for GFAP (G−I) are all mild and similar in tissue immediately adjacent to injections of PBS (B,E,H) or DCH_T (C,F,I). Note also that the architecture of CP tissue immediately adjacent to injection sites of either PBS (K) or DCH_T (L) is indistinguishable in appearance from the characteristic appearance of normal uninjured CP tissue (J). Scale bar = 250 μm for all images.

center of the caudate putamen nucleus, a large homogeneous forebrain structure that is easily targeted and contains neuronal cell bodies intermingled with bundles of myelinated axons and therefore provides a good site to evaluate DCH_T integration with, and effects on, host CNS tissue. In some cases, DCH_T was mixed with small amounts of DCH conjugated with fluorescent blue dye to track hydrogel spread and degradation.

Examination at 1 week after injection showed that DCH_T injected as liquids at room temperature had self-assembled into

single, small, well-formed, ovoid deposits (Figure 3A,E). At 1 week, DCH_T deposits contained few cells (Figure 3A) but by 2 weeks had become filled with cells (Figure 3B) and were well vascularized. Host cells present within the deposits included microglia and astroglia (Figure 4C,F,I), as well as NG2-positive oligodendrocyte progenitor cells and endothelia (data not shown). From 1 to 8 weeks after injection, DCH_T deposits gradually diminished both in size (Figure 3A−D) and fluorescence labeling (Figure 3E−H). At 4 weeks, deposits were small but clearly still present (Figure 3C,G), and by 8 weeks, there was little of the deposits remaining (Figure 3D,H). At all time points, DCH_T deposits caused little disturbance to host tissue cytoarchitecture (Figures 3A−D and 4L). At 8 weeks, when DCH_T deposits had been mostly degraded and absorbed (Figure 3D,H), the appearance of adjacent tissue appeared normal and was indistinguishable from tissue adjacent to injections of PBS or from uninjured tissue (Figure 4J−L). Host tissue gliosis and inflammatory responses to DCH_T deposits were minimal at all times and were indistinguishable from responses to injections of PBS, as demonstrated by staining for Iba1 and CD45 as markers of microglia and inflammatory white blood cells[5] and GFAP as a marker for astrocytes[30] (Figure 4A−I). These findings show that DCH_T injected into healthy CNS tissue self-assemble into well-formed deposits that cause minimal reactive gliosis and are gradually absorbed over time with little residual disturbance to the surrounding normal CNS tissue cytoarchitecture.

3.5. DCH_T Supports NSC Transplanted into the Healthy CNS. Our next objective was to test in a proof-of-concept manner whether these DCH_T could serve as vehicles for transplanting NSC injected into the healthy or injured CNS. As an initial test of DCH_T as carriers for NSC grafts in vivo, we first compared the effects of transplanting NSC into healthy CNS while they were suspended either in culture medium or in our blended DCH_T (Figures 5 and 6). NSCs derived from E11 embryos were expanded in vitro as neurospheres and labeled with GFP. For transplantation, NSCs were suspended at final concentrations of 200 000 cells/μL in either culture media alone or in DCH_T prepared with culture media. Injections consisted of 2 μL (400 000 cells) delivered at a rate of 0.2 μL per minute. As expected, cells suspended in culture medium settled rapidly in the injection cannula and formed concentrated clumps and sedimented rapidly to the bottom of the injection fluid well before the midway point of the injection time (Figure 2C). In contrast, cells remained evenly suspended in the viscous medium of the DCH_T for the entire injection time (Figure 2C). As above (section 3.5), injections were made into the center of the caudate putamen nucleus, which provides a good site to evaluate graft integration with, and effects on, host CNS tissue. Cell grafts were examined at 3 weeks after injection to allow for evaluation of cell survival and integration with and effects on host tissue.

At 3 weeks after injection, GFP-positive NSC transplanted in medium (n = 6 mice) had formed small grafts of densely packed cells that often formed clumps with little or no space between cells (Figures 5A$_{1−5}$ and 6A$_{1−3}$). In contrast, GFP-positive NSC transplanted in DCH_T (n = 6 mice) consistently formed larger deposits in which cells were more evenly distributed and less densely packed with spaces between cell somata in a manner that more closely approximated the cell density of host tissue (Figures 5B$_{1−5}$ and 6B$_{1−3}$). Consistent with these qualitative observations, morphometric graft volume evaluations showed that the mean volume of grafts of GFP-
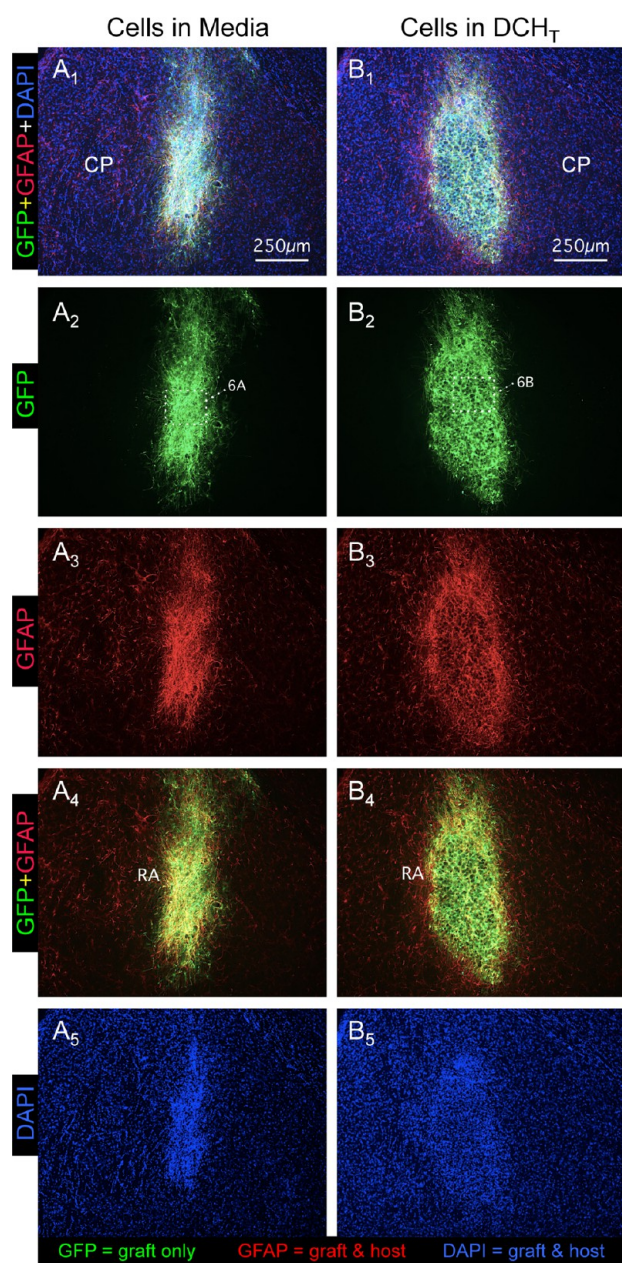
Figure 5. NSC-derived grafts transplanted into uninjured forebrain survive as well or better when injected in DCH_T compared with culture media. (A_{1-5}, B_{1-5}) Images show grafts derived from NSC transplanted into the caudate putamen (CP) nucleus in either culture media (A_{1-5}) or DCH_T (B_{1-5}). The grafts have been stained by triple histofluorescence labeling for the transgenic reporter protein GFP (green), which is expressed only by grafted cells, and the astroglial and progenitor cell marker GFAP (red) and the nuclear marker DAPI, both of which are present in both graft and host cells. Images in A_{1-5} and B_{1-5} show the same fields using different filter combinations. Note that graft transplanted in DCH_T is larger than the graft transplanted in media (A_2, B_2), and that the cells grafted in DCH_T are more evenly spaced and more closely approximate the density of cells in neighboring host tissue (B_5) compared with cells transplanted in media that form a densely packed cluster (A_5). Most grafted cells express both GFP and GFAP under both transplantation conditions (A_4, B_4). Note also that the reactive astrocyte (RA) response is equivalent adjacent to grafts transplanted in media (A_4) or DCH_T (B_4). Boxes in A_2, B_2 indicate areas shown in Figures 6A,B. Scale bar = 250 μm for all images.

positive NSCs transplanted in DCH_T was significantly and approximately 5-fold greater than the mean volume of GFP-positive NSCs transplanted in media (Figure 6C). Morphometric cell number evaluations showed that the mean total number of GFP-positive cells present in grafts of NSC transplanted in DCH_T was significantly and approximately 3-fold that of NSCs transplanted in media (Figure 6C), consistent with the cell clumping and higher packing density of GFP-positive cells in grafts in media. These morphometric cell number evaluations also indicated that at 3 weeks after grafting a mean of about 6% of GFP-positive cells was present relative to the total number of NSCs transplanted in media (23 000 of 400 000 injected cells), whereas a mean of about 18% of the GFP-positive cells was present relative to the total number of NSCs transplanted in DCH_T (72 000 of 400 000 injected cells). These findings indicated significantly enhanced survival of GFP-positive NSCs (or their progeny) injected and transplanted in DCH_T compared with NSCs injected and transplanted in media.

NSC-derived grafts transplanted either in medium or DCH_T interacted equally well with host tissue and caused no evidence of degenerative changes and provoked only minimal reactivity of host astrocytes (Figure $5A_4, B_4$) or microglia (data not shown). With regard to the differentiation of grafted NSCs, no double labeling was found with NeuN as a marker of mature neurons (NeuN)[24] or with GSTπ as a marker of mature oligodendrocytes[25] in grafts transplanted either in medium or DCH_T (data not shown). Instead, double label staining indicated that most GFP-positive, NSC-derived cells in grafts transplanted either in medium or DCH_T also expressed GFAP (Figures $5A_{1-5}, B_{1-5}$ and $6A_{1-5}, 6B_{1-3}$), a marker that labels both astrocytes[30] and neural progenitors.[24] Because GFAP is a marker found in NSC as well as in mature astrocytes,[24,31] we looked for evidence of proliferative activity in NSC-derived grafts in vivo by using BrdU, which is taken up selectively by cells during the S phase of cell division and is commonly used to label proliferating cells in the CNS.[26] BrdU was administered to hosts on days 2−7 after transplantation. Multiple labeling immunohistochemistry showed that a number of GFP- and GFAP-positive cells were also BrdU-positive, indicating that some NSC-derived cells transplanted in DCH_T continued to proliferate during the first days after implantation in vivo (Figure $6C_{1-3}$). Future studies will be required to determine whether graft-derived proliferating cells retain progenitor cell capacity and might be manipulated in their differentiation by molecules simultaneously delivered via DCH_T.

3.6. DCH_T Supports NSC Transplanted into Spinal Cord Injury (SCI) Lesions.

We next tested the effects of DCH_T on NSC transplanted into non-neural lesion core tissue after SCI (Figures 7−9). After traumatic injury in the CNS, lesions form that have different compartments, including central areas of non-neural lesion core tissue, which are surrounded by narrow astrocyte scars that rapidly transition to a perimeter of hypertrophic reactive astrocytes.[5] The central lesion cores of non-neural tissue represent major barriers across which damaged axons do not regrow, thus disconnecting areas of functioning neural tissue. Non-neural lesion core tissue can be targeted by injections of cell grafts or biomaterials, alone or in combination, in an effort to improve neural repair by facilitating host axon regrowth along matrix or cellular bridges that may form new relay connections.[5]

Here, we evaluated the survival and distribution of NSCs suspended in DCH_T and injected into the center of large SCI
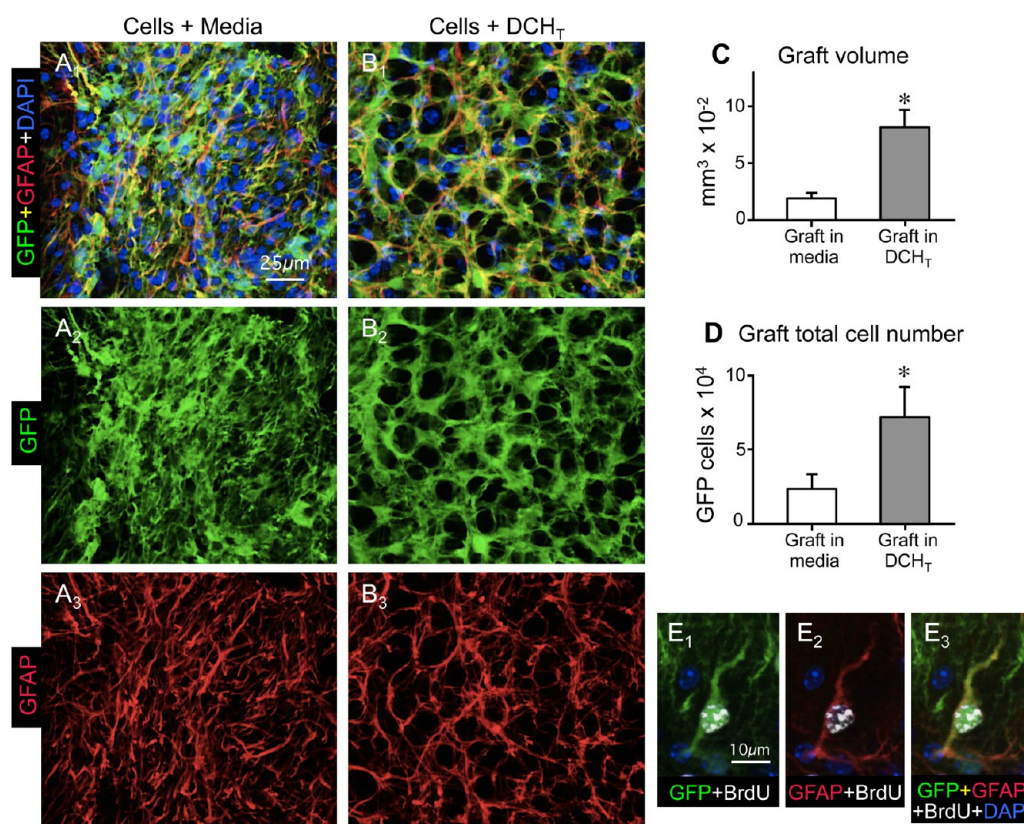
Figure 6. NSC-derived grafts transplanted into uninjured forebrain in DCH_T without added bioactive cargos consist primarily of GFAP-expressing astroglia, some of which retain proliferative potential in vivo. (A_{1-3}, B_{1-3}) Detail images of the boxed areas in Figures $5A_2$, B_2 show that the cells in grafts transplanted in media form densely packed clusters with little or no space between cells (A_{1-3}), whereas cells transplanted in DCH_T are more evenly distributed with spaces between cells (B_{1-3}) in a manner that more closely approximates the distribution of cells in adjacent host CNS tissue. Note that most grafted cells express both GFP and GFAP under both transplantation conditions (A_{1-3}, B_{1-3}). (C) Morphometrically determined mean graft volume of NSC transplanted in DCH_T is significantly greater than that of NSC transplanted in media by approximately 5-fold; $*p < 0.05$ t test ($n = 6$ per group). (D) Morphometrically determined mean total cell number of grafts of NSC transplanted in DCH_T is significantly greater than that of NSC transplanted in media by approximately 3-fold; $*p < 0.05$ t test ($n = 6$ per group). (E_{1-3}) Oil-immersion images of the same cell using different filter combinations show a GFP-labeled, GFAP-expressing, graft-derived cell that exhibits dense nuclear labeling with BrdU, indicating that this cell proliferated sometime between 2 and 7 days after transplantation, during which time BrdU was administered to the host. Scale bars A,B = 50 μm, E = 10 μm.

lesions at 2 days after severe SCI and examined after 3 weeks. For transplantation, NSCs were suspended at final concentrations of 200 000 cells/μL in either culture media alone or in DCH_T prepared with culture media. Injections consisted of 2 μL (400 000 cells) delivered at a rate of 0.2 μL per minute. As discussed above, previous experience indicated that most GFP-positive, NSC-derived cells expressed GFAP after transplantation in vivo. For this reason, as hosts, we used transgenic mGFAP-Cre-tdT mice that expressed the reporter protein tdTomato (tdT) selectively in astroglia,[25] thereby allowing us to differentiate host astroglia labeled violet with tdT, from graft-derived astroglia labeled green with GFP (Figures $7A_{1,2,4}$ and $8A_{1-3}$, B, C_{1-6}). This type of double labeling showed that GFP-labeled NSCs transplanted in DCH_T into large SCI lesions consistently formed grafts of astroglial cells that spread through large areas of the lesion core that contained no host neural cells (Figure $7A_{1-6}$). As in our forebrain grafts (section 3.5), most graft-derived cells in our SCI grafts were GFAP-positive astroglia (Figures $7A_{2,3,5}$ and $8A_{2,4,5}$). Double labeling with GFP and tdTomato also showed that graft-derived GFP-positive immature astroglia migrated for short distances into host tissue (Figures $7A_{1,2,4}$ and $8A_{1-3}$), where they intermingled with host astrocytes (Figure 8B, C_{1-6}) along lesion borders

(Figures $7A_4$ and $8A_3$). Thus, NSC transplanted in DCH_T formed bridges of graft-derived neural tissue that connected areas of host neural tissue widely separated by a non-neural lesion core tissue (Figure $7A_{1-6}$). Morphometric evaluation of GFP-positive cell grafts ($n = 6$ mice), including areas intermingled with a host, showed a mean graft volume of 0.23 ± 0.03 mm^3 and a mean total number of GFP-positive cells per graft of $32\,847 \pm 6468$, indicating that a mean of about 8% of GFP-positive cells was present relative to the 400 000 GFP-positive cells initially injected.

3.7. Growth of Host Axons along Immature Astroglia Derived from NSC Grafted in DCH_T. During CNS development, immature astroglia support axon growth,[32] and transplanted immature astroglia have the potential to promote axon regrowth after SCI.[33] To test whether the NSC-derived immature astroglial cells that we observed after transplantation in DCH_T might support the regrowth of transected host axons into non-neural SCI lesion core tissue, we used immunohistochemical staining for neurofilament M (NFM) to label host axons.[34] All NFM-stained axons could reliably be interpreted as being derived from host neurons because no NFM-positive axons expressed GFP, which labeled all NSC-derived cells.
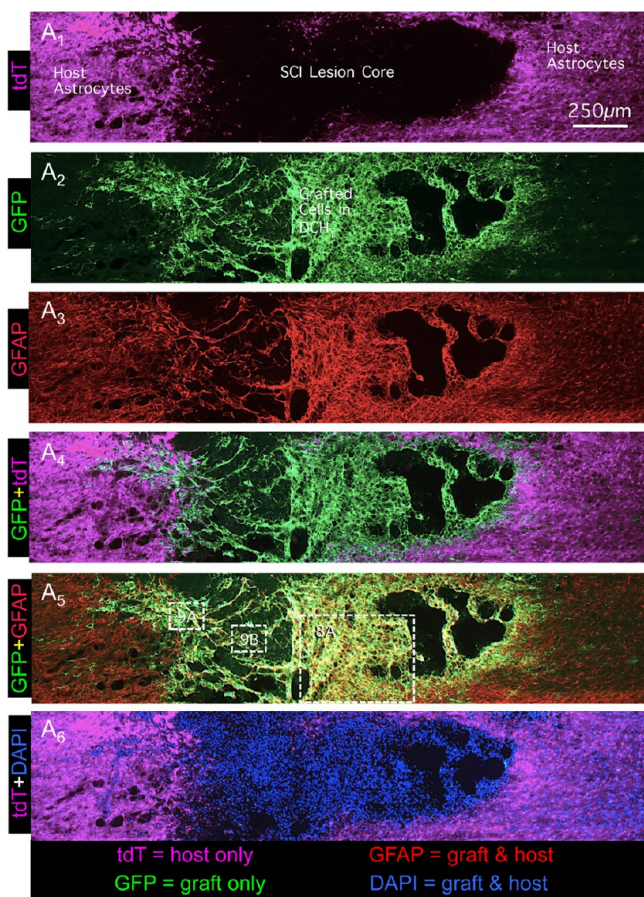
Figure 7. NSCs transplanted in DCH_T into the center of severe spinal cord injury (SCI) can spread throughout large areas of non-neural lesion core tissue and form bridges of graft-derived neural tissue that connect separated areas of host neural tissue. (A_{1-6}) Images show a graft derived from NSCs transplanted in DCH_T into the non-neural lesion core of a SCI at the clinically realistic time of 2 days after injury. The graft has been stained by quadruple histofluorescence labeling for multiple markers including the transgenic reporter protein tdT (violet), which is expressed only by host astrocytes, the transgenic reporter protein GFP (green), which is expressed only by grafted cells, the astroglial and progenitor cell marker GFAP (red) and the nuclear marker DAPI, which are present in both graft and host cells. Images A_{1-6} show the same field using different filter combinations. Note the large SCI lesion that is devoid of host astrocytes but is filled with NSC-derived grafted cells. Note that GFAP is expressed by both grafted and host astroglial cells. Note also the overlap of host and graft-derived astroglia at the borders of the lesion. Boxes in A_5 indicate areas shown at higher magnification in Figures 8A and 9A,B. Scale bar = 250 μm.

In the interface regions between host and graft, many host-derived NFM-positive (and GFP-negative) axons were found in close contact with the surfaces of host astroglia. Some of these axons then clearly transitioned from close contact with host astroglia to close contact with graft-derived astroglia (Figure $9A_{1-3}$). Many NFM-positive axons were observed throughout SCI lesion core areas that were devoid of host neural cells, where the host NFM-positive axons were in close contact with, and appeared to have regrown along, GFP-positive NSC graft-derived immature astroglia (Figure $9B_{1-3}$). Thus, host axons appeared to transition at SCI lesion borders from growth along endogenous astroglia to growth along graft-derived astroglia that extended throughout the lesion cores. The trajectories of most NFM-positive axons in lesion cores appeared to follow

along graft-derived astroglial cell surfaces, resulting in tortuous courses that sometimes completely reversed direction to double back on themselves (Figure $9B_{1-3}$) in a manner that has been used as a criterion for regrowing, as opposed to spared, axons after SCI or other injuries.[35] These findings show that immature astroglia derived from NSCs transplanted in DCH_T into the center of severe SCI lesions can form bridges that support the regrowth of host axons.

4. DISCUSSION

In this study, we showed that nonionic thermoresponsive DCH_T supported the survival of fully immersed and suspended NSCs in vitro in a manner equivalent to cell culture media. At room temperature, NSC suspensions in DCH_T were easily injected into the CNS as liquids, and DCH_T viscosity could be readily tuned to prevent the sedimentation and clumping of suspended NSCs over prolonged times. Suspension in DCH_T significantly and substantively increased the survival of NSCs injected through small-bore cannulae. At body temperature, DCH_T self-assembled into semirigid hydrogels with a stiffness that was readily tuned to that of CNS tissue. In vivo injection of NSCs suspended in DCH_T significantly and substantively increased the cell survival of NSC grafts in the healthy CNS compared with injection of NSCs in culture media. In the injured CNS, NSCs injected as suspensions in DCH_T gave rise to astroglial cells that distributed well throughout non-neural lesion cores, integrated with healthy neural cells at lesion perimeters, and supported the regrowth of host nerve fibers into and through the lesion core that was devoid of host neural cells. Our previous studies show that nonionic DCH_T retains the many advantageous features of our ionic DCH, such as injectability, finely tunable viscosity and rigidity, and the ability to load and provide sustained release of both hydrophilic and hydrophobic molecules. Thus, DCH_T have numerous advantageous properties as vehicles for cell delivery into the CNS for experimental and potential therapeutic applications.

4.1. Improved Survival and Spatial Distribution of NSCs Injected in DCH_T. Low cell survival and poor integration with host tissue are well-recognized hurdles that confront the field of in vivo NSC delivery, and these may be improved by use of biomaterial vehicles.[9] Poor cell survival may result from both technical and biological issues. From a technical perspective, local transplantation of exogenous cells into specific CNS sites is likely to require injection through small-bore cannulae that limit damage to host CNS tissue. Injection of cell suspensions in this manner can be hampered by simple physical factors such as cell sedimentation and clumping before or during the injection process, which in turn can restrict access to nutrients, decrease cell health, and increase cell damage and death due to shear forces during injection.[28,29,36] All of these factors not only can contribute to poor yields of viable cells after injection but also can lead to uneven distribution of transplanted cells within the target host tissue as noted also in this study.

From a technical perspective, our current findings show that nonionic DCH_T offers several features that increase efficiency of NSC transplantation in the CNS. The thermoresponsive characteristics and facile tuning of DCH_T physical properties allow for easy preparation of cell suspensions with tunable viscosity that are liquid and easily injected at room temperature (22 °C) and that self-assemble into well-formed hydrogels with a stiffness tuned to that of CNS tissue at body temperature (37 °C). The viscosity of DCH_T at room temperature was easily
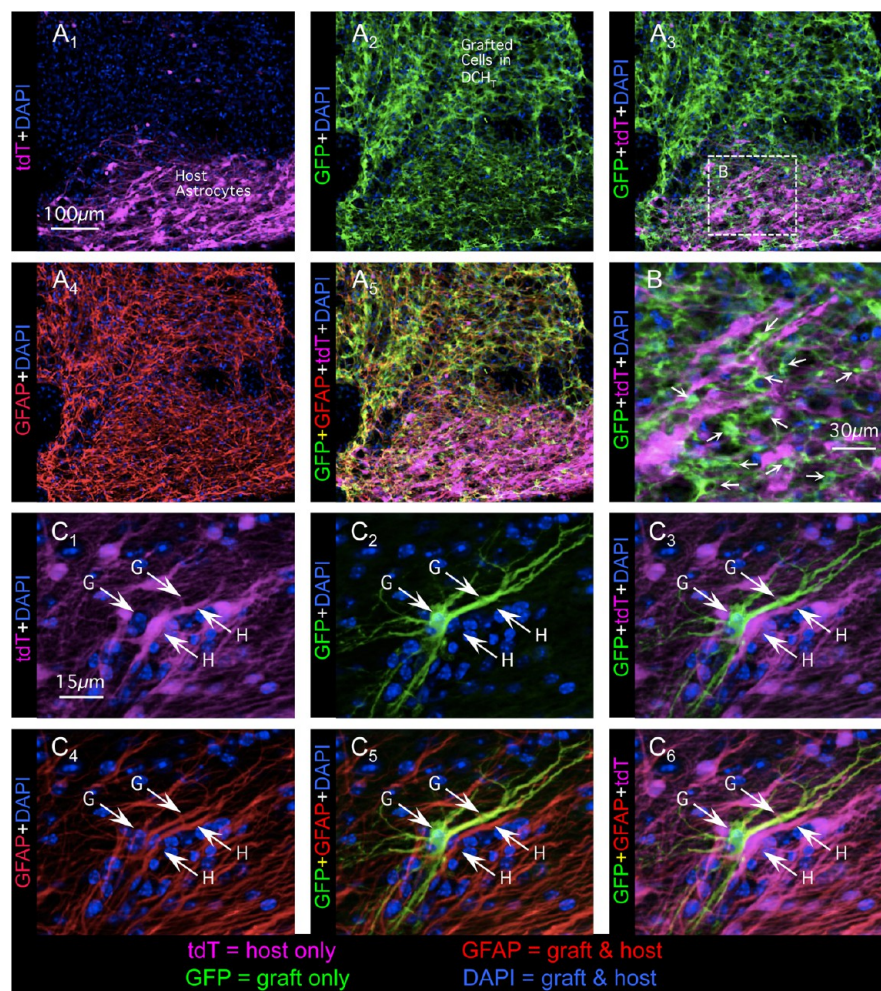
Figure 8. GFAP-positive astroglia derived from NSCs transplanted in DCH_T into the center of severe spinal cord injury (SCI) lesions migrate to intermingle with host astroglia and thereby establish overlapping interfaces of graft and host neural tissue. (A_{1-5}) Images of the area in box labeled 8A in Figure $7A_5$ show the overlap of GFP- and GFAP-positive graft-derived cells with tdT- and GFAP-positive host astroglia in host tissue bordering the graft in the SCI lesion. Images A_{1-5} show the same field using different filter combinations. Box in A_3 indicates area shown at higher magnification in B. (B) Detail of boxed area in A_3 shows intermingling of GFP- and tdT-positive cells. (C_{1-6}) Oil-immersion images of the same field using different filter combinations show the close juxtaposition of a GFP- and GFAP-positive graft-derived (G) astroglia with a tdT- and GFAP-positive host (H) astroglia in host tissue adjacent to the graft. Scale bars A = 100 μm, B = 30 μm, C = 15 μm.

tuned to prevent cell sedimentation over prolonged periods, thereby protecting cells and increasing by 2-fold the survival of NSCs during loading and passage through small-bore cannulae used for CNS injections. NSCs suspended in DCH_T exhibited a significant near 2-fold greater viability immediately after injection through small-bore cannulae compared with NSCs injected in culture media only. In addition, cells injected in DCH_T in vivo exhibited a more even distribution of transplanted cells, whereas NSC injected in culture media formed dense clumps. Together, these factors resulted in a significant 3-fold increase from about 6% of the total number of GFP-positive cells injected surviving at 3 weeks after grafting relative to the total number of NSCs transplanted in media to 18% of GFP-positive cells surviving relative to the total number of NSCs transplanted in DCH_T. Notably, this increase was achieved without addition of exogenous growth factors or other bioactive molecules, which may have the potential to further increase the number of surviving transplanted cells in future studies.

It is also noteworthy that NSC grafts transplanted in DCH_T after CNS injury dispersed well in lesion sites, and that grafted cells interfaced well and intermingled with host cells at lesion borders to form host−graft transition zones. The mean volume of DCH_T-supported grafts placed into SCI tissue was larger by about one-third compared with DCH_T-supported grafts in healthy forebrain tissue, suggesting that DCH_T-supported grafts might spread more readily in damaged tissue, perhaps because damaged tissue is less stiff and offers less resistance, a point for future investigation. Nevertheless, we also found that the number of GFP-positive DCH_T-supported GFP-positive cells surviving at 3 weeks after grafting into SCI lesions was only about 8% of the total number of GFP-positive cells injected, which was less than half of the 18% surviving after grafting into healthy forebrain tissue. In this regard, our observations are consistent with findings of others who report that the inflammatory environment of subacutely damaged CNS tissue is hostile to grafted cells compared with healthy CNS tissue and that biomaterial carriers can increase the survival of grafted cells.[2−4,9] As information about different biomaterial carriers accrues, it will be interesting in future studies to compare different carriers. Because DCH_T can be loaded with diverse molecular cargos, it will also be interesting to test in future
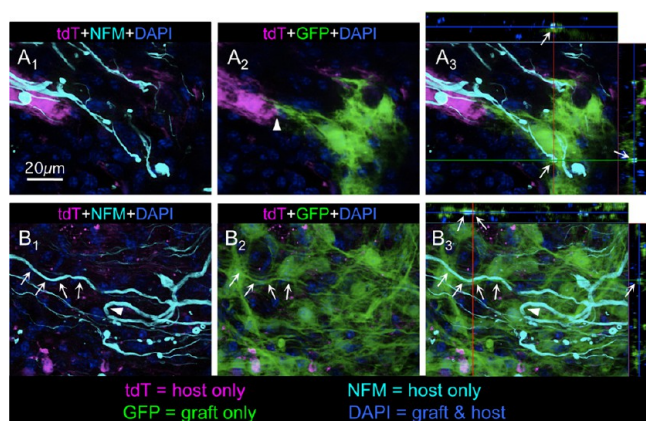
Figure 9. Astroglia derived from NSCs transplanted in DCH_T into the center of severe spinal cord injury (SCI) lesions can support the regrowth of host axons that transition from endogenous astroglia to graft-derived astroglia at SCI lesion borders and grow along graft-derived astroglia in SCI lesion core areas devoid of host neural cells. (A_{1-3}) Oil-immersion images of the same field using different filter combinations show NFM-positive host axons that are in direct contact with both host tdT-positive astroglia and graft-derived GFP-positive astroglia in a transition zone where there is overlap of host and graft-derived astroglia at the border to the SCI lesion demarcated by the box labeled 9A in Figure $7A_5$. Arrowhead in $9A_2$ indicates transition point of an axon from a host astroglia to a graft-derived astroglia. Arrows in the three-dimensional ortho-image $9A_3$ indicate the direct contact of a host axon with the surface of a graft-derived astroglia. (B_{1-3}) Oil-immersion images of the same field using different filter combinations show NFM-positive host axons that are in direct contact with graft-derived GFP-positive astroglia in the center of an SCI lesion demarcated by the box labeled 9B in Figure $7A_5$. Arrowhead indicates a host axon that reverses its direction, which is regarded a hallmark of regenerating axons. Arrows indicate the direct contact of a host axon with the surface of a graft-derived astroglia. Scale bar = 20 μm for all images.

studies whether such molecular delivery can improve the survival or otherwise modulate grafted cells.

4.2. Potential for Simultaneous Manipulation in Vivo of Both Host and Grafted Cells Using DCH_T. Another current limitation in transplantation of NSCs into the CNS is the lack of ability to regulate NSC maturation and integration with host cells.[9] During neural development in vivo, NSCs mature and organize into functional units over prolonged times in a manner that is regulated and guided by exposure to different molecules at different times. These temporally and spatially regulated molecular cues are for the most part lacking in the mature injured or diseased CNS that is the main target of NSC transplantation. Biomaterial vehicles have the potential to facilitate in vivo NSC delivery strategies by co-delivery of bioactive molecules that act on grafted NSC or on host tissue.[9] With regard to the capacity for co-delivery of NSCs and bioactive molecules, DCH_T compares favorably with other biomaterials being tested as NSC vehicles, such as fibrin, poly(ε-caprolactone), hyaluran/methylcellulose, collagens, and others.[9] As shown here, DCH_T improves the survival of grafted NSCs. As demonstrated previously, DCH_T exhibits good capacity for molecular delivery of both hydrophilic and hydrophobic molecules[18] in a manner similar to other DCHs, which can provide sustained release of hydrophilic growth factors[7] and hydrophobic manipulators of gene expression or epigenetic mechanisms.[15] Few other biomaterials have this dual capacity for hydrophilic and hydrophobic molecular delivery.

Loading of DCH_T with regulatory cargo molecules has the potential to (i) improve the survival of NSC grafted into inflamed and hostile damaged CNS tissue, (ii) modulate the differentiation of NSC after transplantation in vivo, and (iii) facilitate the appropriate integration of NSC-derived progeny with host cells. In addition, DCH_T offers the possibility of delivering molecules that may influence host cells to promote repair and recovery. For example, a number of different growth factors are now recognized as being able to stimulate and attract the regrowth of specific types of axons,[1,37,38] and molecular regulators of intrinsic neuronal capacity for axon growth are being identified.[39,40] Providing or modulating such factors via DCH_T could improve regrowth of axons into, through, and out of grafts of transplanted NSCs. In this regard, it is important to note that DCH_T caused little detectable long-term effects after injection into healthy CNS tissue, indicating that DCH_T depots (without cell grafts) could be injected into healthy CNS in an effort either to stimulate regeneration promoting genetic programs or to attract regenerating axons into regions that have target neurons with which they might form new connections. Thus, DCH_T provides a powerful new tool for experimental investigation of cellular and molecular mechanisms during the study of CNS injury and repair in vivo.

4.3. Potential for DCH_T To Facilitate Regrowth of Host Axons along Grafted Cells across CNS Lesions. CNS lesions that form after severe tissue damage are characterized by non-neural lesion core tissue (also referred to as fibrotic scar) and fluid-filled cysts that are surrounded by compact borders of an astroglial scar.[5,41,42] Human SCI, in particular, is characterized by large areas of non-neural fibrotic scar tissue and cysts that can extend over long distances.[43] This non-neural scar tissue is exquisitely hostile to regrowth of damaged host axons. Facilitating host axon regrowth to re-establish connectivity across such lesions is a complex challenge. Although astrocyte scars are commonly regarded as inhibitory to axon regrowth after CNS injury,[44] in the developing CNS, immature astroglia robustly support axon growth.[32] After SCI, transected axons that are stimulated to grow by genetic manipulations appear to grow along astrocyte bridges when these are present in CNS lesions, whereas these stimulated axons do not grow among non-neural lesion core cells.[40] Re-establishing neuronal connections across such non-neural lesion core tissue is a long sought after research goal. There is growing evidence that formation of new relay circuits has the potential to re-establish certain forms of function after CNS injury, and that achieving even short distance axon regrowth can lead to formation of relay circuits.[45,46] Grafts of NSCs that generate either neurons or neural glial cells are being explored as potential means of facilitating the formation of new relay connections. There is evidence that NSCs transplanted into lesions can generate new neurons that form new functional relays.[1,2,47] In addition, grafted NSCs that give rise to newly generate immature astroglial cells have the potential to form bridges that can enable host axons to regrow across tissue lesions and thereby form new relays.[33,48,49] Our current findings show that NSCs suspended in DCH_T blend and injected into lesion sites after SCI distribute well and give rise to progeny cells throughout the non-neural lesion core and intermingle with host neural cells at lesion edges, thereby forming potential bridges of neural cells across lesions. We also found that grafted, NSC-derived immature astroglia in DCH_T supported the transition of regrowing host axons from growth along host astroglia to growth along graft astroglia that

extended throughout lesion core tissue. These findings add to other evidence that grafts of neural lineage cells, including immature astroglia, can support the growth of axons through CNS tissue lesions that would otherwise present an environment hostile to such growth.[48,49] Combining the ability of DCH$_T$ to simultaneously deliver cells and molecules may be a promising approach to test the potential for NSC grafts to give rise to neural cells that form bridges for promoting axon regrowth across non-neural CNS lesions.

5. CONCLUSIONS

In this study, we have extended the utility of DCH for CNS applications to encompass that of serving as vehicles for transplantation of cell suspensions into the healthy and injured CNS. Nonionic, thermoresponsive DCH$_T$ exhibited excellent cytocompatibility and supported the long-term viability of suspended cells in vitro while retaining the many advantageous features of our previously studied ionic DCH, such as injectability, tunable viscosity, and rigidity, as well as the previously demonstrated ability to load and provide sustained release of both hydrophilic and hydrophobic molecules. The thermoresponsiveness of DCH$_T$ allowed facile preparation of cell suspensions that were easily injected liquids at room temperature and that self-assembled into well-formed hydrogels at body temperature that were tuned to the stiffness of CNS tissue. DCH$_T$ significantly and markedly increased the survival of NSC injected through small-bore cannulae and grafted into the CNS. NSCs injected in DCH$_T$ into the injured CNS gave rise to new neural cells that distributed throughout large tissue lesions and supported the regrowth of host nerve fibers into and through lesion core tissue that was devoid of host neural cells. Our findings indicate that nonionic DCH$_T$ has the potential to become a powerful new tool for in vivo delivery of cells and molecules in the CNS for experimental investigations and potential therapeutic strategies.

■ AUTHOR INFORMATION

Corresponding Author
*Tel.: +1 310 794 4944. E-mail: sofroniew@mednet.ucla.edu.

Author Contributions
⊥S.Z., J.E.B., and M.A.A. contributed equally to this work.

Notes
The authors declare no competing financial interest.

■ ACKNOWLEDGMENTS

■ REFERENCES

(1) Bonner, J. F.; Connors, T. M.; Silverman, W. F.; Kowalski, D. P.; Lemay, M. A.; Fischer, I. Grafted neural progenitors integrate and restore synaptic connectivity across the injured spinal cord. *J. Neurosci.* **2011**, *31* (12), 4675−86.

(2) Lu, P.; Wang, Y.; Graham, L.; McHale, K.; Gao, M.; Wu, D.; Brock, J.; Blesch, A.; Rosenzweig, E. S.; Havton, L. A.; Zheng, B.; Conner, J. M.; Marsala, M.; Tuszynski, M. H. Long-distance growth and connectivity of neural stem cells after severe spinal cord injury. *Cell* **2012**, *150* (6), 1264−73.

(3) Lemmens, R.; Steinberg, G. K. Stem cell therapy for acute cerebral injury: what do we know and what will the future bring? *Curr. Opin. Neurol.* **2013**, *26* (6), 617−25.

(4) Dunnett, S. B.; Rosser, A. E. Challenges for taking primary and stem cells into clinical neurotransplantation trials for neurodegenerative disease. *Neurobiol. Dis.* **2014**, *61*, 79−89.

(5) Burda, J. E.; Sofroniew, M. V. Reactive gliosis and the multicellular response to CNS damage and disease. *Neuron* **2014**, *81* (2), 229−48.

(6) Pakulska, M. M.; Ballios, B. G.; Shoichet, M. S. Injectable hydrogels for central nervous system therapy. *Biomed. Mater.* **2012**, *7* (2), 024101.

(7) Song, B.; Song, J.; Zhang, S.; Anderson, M. A.; Ao, Y.; Yang, C. Y.; Deming, T. J.; Sofroniew, M. V. Sustained local delivery of bioactive nerve growth factor in the central nervous system via tunable diblock copolypeptide hydrogel depots. *Biomaterials* **2012**, *33* (35), 9105−16.

(8) Hoban, D. B.; Newland, B.; Moloney, T. C.; Howard, L.; Pandit, A.; Dowd, E. The reduction in immunogenicity of neurotrophin overexpressing stem cells after intra-striatal transplantation by encapsulation in an in situ gelling collagen hydrogel. *Biomaterials* **2013**, *34* (37), 9420−9.

(9) Elliott Donaghue, I.; Tam, R.; Sefton, M. V.; Shoichet, M. S. Cell and biomolecule delivery for tissue repair and regeneration in the central nervous system. *J. Controlled Release* **2014**, *190*, 219−27.

(10) Yang, C. Y.; Song, B.; Ao, Y.; Nowak, A. P.; Abelowitz, R. B.; Korsak, R. A.; Havton, L. A.; Deming, T. J.; Sofroniew, M. V. Biocompatibility of amphiphilic diblock copolypeptide hydrogels in the central nervous system. *Biomaterials* **2009**, *30* (15), 2881−2898.

(11) Deming, T. J. Polypeptide hydrogels via a unique assembly mechanism. *Soft Matter* **2005**, *1*, 28−35.

(12) Deming, T. J. Facile synthesis of block copolypeptides of defined architecture. *Nature* **1997**, *390* (6658), 386−389.

(13) Nowak, A. P.; Breedveld, V.; Pakstis, L.; Ozbas, B.; Pine, D. J.; Pochan, D.; Deming, T. J. Rapidly recovering hydrogel scaffolds from self-assembling diblock copolypeptide amphiphiles. *Nature* **2002**, *417*, 424−428.

(14) Breedveld, V.; Nowak, A. P.; Sato, J.; Deming, T. J.; Pine, D. J. Rheology of block copolypeptide solutions: hydrogels with tunable properties. *Macromolecules* **2004**, *37*, 3943−3953.

(15) Zhang, S.; Anderson, M. A.; Ao, Y.; Khakh, B. S.; Fan, J.; Deming, T. J.; Sofroniew, M. V. Tunable diblock copolypeptide hydrogel depots for local delivery of hydrophobic molecules in healthy and injured central nervous system. *Biomaterials* **2014**, *35* (6), 1989−2000.

(16) Chilkoti, A.; Dreher, M. R.; Meyer, D. E.; Raucher, D. Targeted drug delivery by thermally responsive polymers. *Adv. Drug Delivery Rev.* **2002**, *54* (5), 613−30.

(17) Klouda, L.; Mikos, A. G. Thermoresponsive hydrogels in biomedical applications. *Eur. J. Pharm. Biopharm.* **2008**, *68* (1), 34−45.

(18) Zhang, S.; Alvarez, D. J.; Sofroniew, M. V.; Deming, T. J. Design and synthesis of nonionic copolypeptide hydrogels with reversible thermoresponsive and tunable physical properties. *Biomacromolecules* **2015**, *16* (4), 1331−40.

(19) Reynolds, B. A.; Weiss, S. Generation of neurons and astrocytes from isolated cells of the adult mammalian central nervous system. *Science* **1992**, *255*, 1707−1710.

(20) Singec, I.; Knoth, R.; Meyer, R. P.; Maciaczyk, J.; Volk, B.; Nikkhah, G.; Frotscher, M.; Snyder, E. Y. Defining the actual sensitivity and specificity of the neurosphere assay in stem cell biology. *Nat. Methods* **2006**, *3* (10), 801−6.

(21) Conti, L.; Pollard, S. M.; Gorba, T.; Reitano, E.; Toselli, M.; Biella, G.; Sun, Y.; Sanzone, S.; Ying, Q. L.; Cattaneo, E.; Smith, A. Niche-independent symmetrical self-renewal of a mammalian tissue stem cell. *PLoS Biol.* **2005**, *3* (9), e283.

(22) Kramer, J. R.; Rodriguez, A. R.; Choe, U. J.; Kamei, D. T.; Deming, T. J. Glycopolypeptide conformations in bioactive block copolymer assemblies influence their nanoscale morphology. *Soft Matter* **2013**, *9* (12), 3389−3395.

(23) Madisen, L.; Zwingman, T. A.; Sunkin, S. M.; Oh, S. W.; Zariwala, H. A.; Gu, H.; Ng, L. L.; Palmiter, R. D.; Hawrylycz, M. J.; Jones, A. R.; Lein, E. S.; Zeng, H. A robust and high-throughput Cre

reporting and characterization system for the whole mouse brain. *Nat. Neurosci.* **2010**, *13* (1), 133−140.

(24) Garcia, A. D. R.; Doan, N. B.; Imura, T.; Bush, T. G.; Sofroniew, M. V. GFAP-expressing progenitors are the principle source of constitutive neurogenesis in adult mouse forebrain. *Nat. Neurosci.* **2004**, *7*, 1233−1241.

(25) Herrmann, J. E.; Imura, T.; Song, B.; Qi, J.; Ao, Y.; Nguyen, T. K.; Korsak, R. A.; Takeda, K.; Akira, S.; Sofroniew, M. V. STAT3 is a critical regulator of astrogliosis and scar formation after spinal cord injury. *J. Neurosci.* **2008**, *28* (28), 7231−7243.

(26) Wanner, I. B.; Anderson, M. A.; Song, B.; Levine, J.; Fernandez, A.; Gray-Thompson, Z.; Ao, Y.; Sofroniew, M. V. Glial scar borders are formed by newly proliferated, elongated astrocytes that interact to corral inflammatory and fibrotic cells via STAT3-dependent mechanisms after spinal cord injury. *J. Neurosci.* **2013**, *33* (31), 12870−86.

(27) Faulkner, J. R.; Herrmann, J. E.; Woo, M. J.; Tansey, K. E.; Doan, N. B.; Sofroniew, M. V. Reactive astrocytes protect tissue and preserve function after spinal cord injury. *J. Neurosci.* **2004**, *24*, 2143−2155.

(28) Aguado, B. A.; Mulyasasmita, W.; Su, J.; Lampe, K. J.; Heilshorn, S. C. Improving viability of stem cells during syringe needle flow through the design of hydrogel cell carriers. *Tissue Eng., Part A* **2012**, *18* (7−8), 806−815.

(29) Yan, C.; Mackay, M. E.; Czymmek, K.; Nagarkar, R. P.; Schneider, J. P.; Pochan, D. J. Injectable solid peptide hydrogel as a cell carrier: effects of shear flow on hydrogels and cell payload. *Langmuir* **2012**, *28* (14), 6076−87.

(30) Sofroniew, M. V.; Vinters, H. V. Astrocytes: biology and pathology. *Acta Neuropathol.* **2010**, *119* (1), 7−35.

(31) Kriegstein, A.; Alvarez-Buylla, A. The glial nature of embryonic and adult neural stem cells. *Annu. Rev. Neurosci.* **2009**, *32*, 149−184.

(32) Norris, C. R.; Kalil, K. Guidance of callosal axons by radial glia in the developing cerebral cortex. *J. Neurosci.* **1991**, *11* (11), 3481−3492.

(33) Hasegawa, K.; Chang, Y. W.; Li, H.; Berlin, Y.; Ikeda, O.; Kane-Goldsmith, N.; Grumet, M. Embryonic radial glia bridge spinal cord lesions and promote functional recovery following spinal cord injury. *Exp. Neurol.* **2005**, *193* (2), 394−410.

(34) Inman, D. M.; Steward, O. Ascending sensory, but not other long-tract axons, regenerate into the connective tissue matrix that forms at the site of a spinal cord injury in mice. *J. Comp. Neurol.* **2003**, *462* (4), 431−49.

(35) Tuszynski, M. H.; Steward, O. Concepts and methods for the study of axonal regeneration in the CNS. *Neuron* **2012**, *74* (5), 777−91.

(36) Lu, H. D.; Charati, M. B.; Kim, I. L.; Burdick, J. A. Injectable shear-thinning hydrogels engineered with a self-assembling Dock-and-Lock mechanism. *Biomaterials* **2012**, *33* (7), 2145−53.

(37) Iannotti, C.; Li, H.; Yan, P.; Lu, X.; Wirthlin, L.; Xu, X. M. Glial cell line-derived neurotrophic factor-enriched bridging transplants promote propriospinal axonal regeneration and enhance myelination after spinal cord injury. *Exp. Neurol.* **2003**, *183* (2), 379−393.

(38) McCall, J.; Weidner, N.; Blesch, A. Neurotrophic factors in combinatorial approaches for spinal cord regeneration. *Cell Tissue Res.* **2012**, *349* (1), 27−37.

(39) Liu, K.; Tedeschi, A.; Park, K. K.; He, Z. Neuronal intrinsic mechanisms of axon regeneration. *Annu. Rev. Neurosci.* **2011**, *34*, 131−52.

(40) Zukor, K.; Belin, S.; Wang, C.; Keelan, N.; Wang, X.; He, Z. Short hairpin RNA against PTEN enhances regenerative growth of corticospinal tract axons after spinal cord injury. *J. Neurosci.* **2013**, *33* (39), 15350−61.

(41) Fernandez-Klett, F.; Priller, J. The fibrotic scar in neurological disorders. *Brain Pathol.* **2014**, *24* (4), 404−13.

(42) Sofroniew, M. V. Astrocyte barriers to neurotoxic inflammation. *Nat. Rev. Neurosci.* **2015**, *16* (5), 249−63.

(43) Norenberg, M. D.; Smith, J.; Marcillo, A. The pathology of human spinal cord injury: defining the problems. *J. Neurotrauma* **2004**, *21* (4), 429−40.

(44) Silver, J.; Miller, J. H. Regeneration beyond the glial scar. *Nat. Rev. Neurosci.* **2004**, *5*, 146−156.

(45) Bareyre, F. M.; Kerschensteiner, M.; Raineteau, O.; Mettenleiter, T. C.; Weinmann, O.; Schwab, M. E. The injured spinal cord spontaneously forms a new intraspinal circuit in adult rats. *Nat. Neurosci.* **2004**, *7*, 269−277.

(46) Courtine, G.; Song, B.; Roy, R. R.; Zhong, H.; Herrmann, J. E.; Ao, Y.; Qi, J.; Edgerton, V. R.; Sofroniew, M. V. Recovery of supraspinal control of stepping via indirect propriospinal relay connections after spinal cord injury. *Nat. Med.* **2008**, *14* (1), 69−74.

(47) Abematsu, M.; Tsujimura, K.; Yamano, M.; Saito, M.; Kohno, K.; Kohyama, J.; Namihira, M.; Komiya, S.; Nakashima, K. Neurons derived from transplanted neural stem cells restore disrupted neuronal circuitry in a mouse model of spinal cord injury. *J. Clin. Invest.* **2010**, *120* (9), 3255−66.

(48) Williams, R. R.; Henao, M.; Pearse, D. D.; Bunge, M. B. Permissive Schwann cell graft/spinal cord interfaces for axon regeneration. *Cell Transplant* **2015**, *24* (1), 115−131.

(49) Chu, T.; Zhou, H.; Li, F.; Wang, T.; Lu, L.; Feng, S. Astrocyte transplantation for spinal cord injury: Current status and perspective. *Brain Res. Bull.* **2014**, *107*, 18−30.